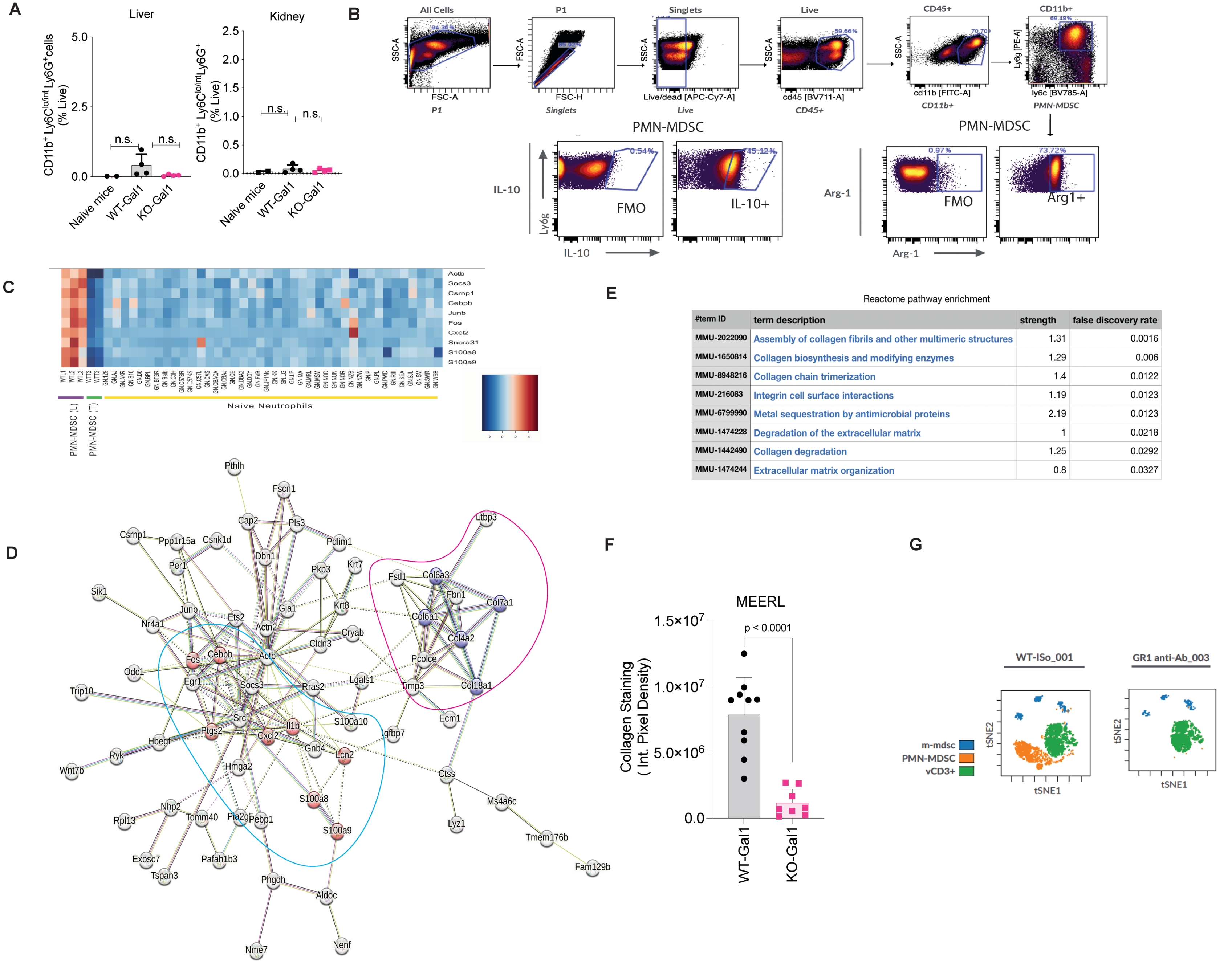

#term ID	term description	strength	false discovery rate
MMU-2022090	Assembly of collagen fibrils and other multimeric structures	1.31	0.0016
MMU-1650814	Collagen biosynthesis and modifying enzymes	1.29	0.006
MMU-8948216	Collagen chain trimerization	1.4	0.0122
MMU-216083	Integrin cell surface interactions	1.19	0.0123
MMU-6799990	Metal sequestration by antimicrobial proteins	2.19	0.0123
MMU-1474228	Degradation of the extracellular matrix	1	0.0218
MMU-1442490	Collagen degradation	1.25	0.0292
MMU-1474244	Extracellular matrix organization	0.8	0.0327

Supplementary Figure 3: A. Quantification of PMN-MDSCs (CD11b+Ly6Clo/intLy6G+) in the liver and kidneys of MOC2 WT- or KO-Gal1 tumor-bearing mice at matched tumor volumes in comparison with naïve mice. **B.** Gating strategy used to quantify Arginase (Arg1) and interleukin-10 (IL-10) expression on PMN-MDSCs isolated from the tumor or the lungs of naïve mice or mice with pre-metastatic niches (sub-gated on CD45+ live cells). **C.** Heat map showing differential gene expression from PMN-MDSCs isolated from tumor and lung tissues of MOC2 WT-Gal1 tumor-bearing mice compared with naïve neutrophils. **D.** STRING analysis showing two clusters of genes representing IL-17 and collagen synthesis pathways that are upregulated PMN-MDSCs isolated from pre-metastatic lung tissues. **E.** Reactome pathway enrichment analyses performed using RNA-SEQ data showing pathway represented by upregulated genes in PMN-MDSCs isolated from pre-metastatic lung tissues. **F.** Quantification of Trichrome staining intensity in mEERL WT- or KO-Gal1 tumor-bearing mice lungs, n=5/group. **G.** tSNE plot showing depletion of PMN-MDSCs in the blood following injection of anti-GR1 antibody in mice compared with isotype alone.

SUPPLEMENTARY FIGURE: 3